

Supplementary information

Prediction of orientation relationships and interface structures between α -, β -, γ -FeSi₂ and Si phases

M.A.Visotin^{*a,b}, I.A. Tarasov^a, A.S. Fedorov^{a,b}, S.N. Varnakov^a, S.G. Ovchinnikov^{a,b}

^aKirensky Institute of Physics, Federal Research Center KSC SB RAS, Krasnoyarsk, 660036 Russia

^bSiberian Federal University, 660041, Krasnoyarsk, Russia

*Corresponding author.

E-mail address: mav@iph.krasn.ru (Maxim A. Visotin).

S1. Additional data on α -, β -, γ -FeSi₂ and Si interface prediction

Table S1 The list of crystallographic vectors in the phases considered with the packing density calculated. The close-packed directions are highlighted.

Phase	Si		α -FeSi ₂		β -FeSi ₂		γ -FeSi ₂	
Ranking number	Direction Row packing density							
1	[110]	0.26041	[001]	0.39002	[100]	0.40501	[100]	0.37113
2	[111]	0.21263	[100]	0.37258	[010]	0.25646	[111]	0.32141
3	[100]	0.18414	[221]	0.32747	[001]	0.25524	[110]	0.26243
4	[114]	0.17361	[201]	0.26941	[120]	0.21667	[411]	0.17495
5	[332]	0.15703	[110]	0.26345	[201]	0.18823	[311]	0.16785
6	[211]	0.15035	[223]	0.17488	[022]	0.18091	[210]	0.16597
7	[433]	0.12632	[101]	0.17277	[021]	0.17187	[332]	0.15825
8	[611]	0.11948	[621]	0.16918	[012]	0.17138	[211]	0.15151
9	[310]	0.11104	[401]	0.16810	[220]	0.15893	[530]	0.12730
10	[552]	0.10023	[210]	0.16662	[111]	0.13491	[221]	0.12371
11	[321]	0.09843	[111]	0.15674	[031]	0.12159	[611]	0.12041
12	[732]	0.09354	[302]	0.15338	[013]	0.12113	[310]	0.11736
13	[811]	0.09066	[421]	0.15323	[114]	0.11843	[710]	0.10497
14	[322]	0.08932	[551]	0.15260	[312]	0.11623	[543]	0.10497
15	[331]	0.08449	[501]	0.13921	[131]	0.11288	[320]	0.10293
16	[210]	0.08235	[412]	0.13256	[113]	0.11251	[551]	0.10101
17	[833]	0.08134	[332]	0.13051	[102]	0.10797	[321]	0.09919
18	[932]	0.07597	[521]	0.13051	[121]	0.09973	[730]	0.09746
19	[941]	0.07440	[103]	0.12807	[112]	0.09951	[732]	0.09427
20	[510]	0.07220	[530]	0.12779	[332]	0.09786	[510]	0.07278
21	[521]	0.06724	[211]	0.12668	[210]	0.09418	[431]	0.07278
22	[530]	0.06316	[113]	0.12622	[152]	0.09266	[521]	0.06776
23	[532]	0.05974	[441]	0.12480	[314]	0.09126	[532]	0.06021
24	[541]	0.05683	[610]	0.12250	[211]	0.08836	[541]	0.05727
25	[631]	0.05430	[502]	0.11841	[122]	0.08259	[631]	0.05472

Table S2 Top 20 (of 556) predicted coherent interfaces between silicon and $\beta\text{-FeSi}_2$ iron silicide (raw data).

Ranking number	(hkl)	(hkl)	[uvw]	[uvw]	δ_1 , close-packed direction misfit, %	R, NCS density	$\tilde{\varepsilon}$, strain, %
$\beta\text{-FeSi}_2 \parallel \text{Si}$							
i.1	$\beta(10-1)$	Si(1-1-1)	$\beta[010]$	Si[110]	1.54	0.75	2.47
i.2	$\beta(-110)$	Si(1-1-1)	$\beta[001]$	Si[110]	2.03	0.75	2.51
i.3	$\beta(100)$	Si(00-1)	$\beta[010]$	Si[110]	1.54	0.70	1.52
i.4	$\beta(-100)$	Si(001)	$\beta[011]$	Si[200]	1.78	0.70	1.52
i.5	$\beta(100)$	Si(001)	$\beta[011]$	Si[200]	1.78	0.70	1.52
i.6	$\beta(-100)$	Si(00-1)	$\beta[001]$	Si[110]	2.03	0.70	1.52
i.7	$\beta(-310)$	Si(1-1-3)	$\beta[002]$	Si[220]	2.03	0.57	0.93
i.8	$\beta(-11-1)$	Si(0-12)	$\beta[011]$	Si[200]	1.78	0.54	3.30
i.9	$\beta(-510)$	Si(1-1-5)	$\beta[001]$	Si[110]	2.03	0.51	1.24
i.10	$\beta(00-1)$	Si(1-10)	$\beta[010]$	Si[110]	1.54	0.48	4.65
i.11	$\beta(00-1)$	Si(01-1)	$\beta[120]$	Si[222]	-1.87	0.47	4.65
i.12	$\beta(001)$	Si(-1-10)	$\beta[120]$	Si[222]	-1.87	0.47	4.65
i.13	$\beta(31-1)$	Si(0-23)	$\beta[011]$	Si[200]	1.78	0.46	0.82
i.14	$\beta(51-1)$	Si(0-25)	$\beta[011]$	Si[200]	1.78	0.46	0.98
i.15	$\beta(-210)$	Si(1-1-2)	$\beta[001]$	Si[110]	2.03	0.45	0.97
i.16	$\beta(-53-3)$	Si(0-56)	$\beta[011]$	Si[200]	1.78	0.45	2.05
i.17	$\beta(2-10)$	Si(-12-1)	$\beta[120]$	Si[222]	-1.87	0.45	0.97
i.18	$\beta(71-1)$	Si(0-27)	$\beta[011]$	Si[200]	1.79	0.45	1.21
i.19	$\beta(4-2-1)$	Si(-34-1)	$\beta[120]$	Si[222]	-1.87	0.44	1.10
i.20	$\beta(4-21)$	Si(-14-3)	$\beta[120]$	Si[222]	-1.87	0.43	1.10

Table S3 Top 20 (of 4535) predicted coherent interfaces between silicon and α -FeSi₂ iron silicide (raw data).

Ranking number	(hkl)	(hkl)	[uvw]	[uvw]	δ_1 , close-packed direction misfit, %	R, NCS density	$\tilde{\varepsilon}$, strain, %
α-FeSi₂ Si							
i.1	$\alpha(-112)$	Si(1-1-1)	$\alpha[201]$	Si[110]	-2.97	0.90	2.15
i.2	$\alpha(-2-14)$	Si(1-1-3)	$\alpha[201]$	Si[110]	-2.97	0.79	6.74
i.3	$\alpha(1-1-1)$	Si(1-1-3)	$\alpha[220]$	Si[110]	-0.73	0.76	8.23
i.4	$\alpha(00-1)$	Si(00-1)	$\alpha[220]$	Si[110]	-0.73	0.75	0.64
i.5	$\alpha(1-1-2)$	Si(1-1-1)	$\alpha[220]$	Si[110]	-0.73	0.75	2.15
i.6	$\alpha(010)$	Si(00-1)	$\alpha[201]$	Si[110]	-2.97	0.75	2.98
i.7	$\alpha(0-10)$	Si(00-1)	$\alpha[201]$	Si[110]	-2.97	0.75	2.98
i.8	$\alpha(-1-12)$	Si(1-1-1)	$\alpha[201]$	Si[110]	-2.97	0.75	2.15
i.9	$\alpha(001)$	Si(001)	$\alpha[200]$	Si[100]	-0.73	0.75	0.64
i.10	$\alpha(0-10)$	Si(001)	$\alpha[200]$	Si[100]	-0.73	0.75	2.98
i.11	$\alpha(-1-32)$	Si(1-1-3)	$\alpha[201]$	Si[110]	-2.97	0.59	2.75
i.12	$\alpha(-214)$	Si(1-1-3)	$\alpha[201]$	Si[110]	-2.97	0.59	6.74
i.13	$\alpha(1-1-6)$	Si(1-1-3)	$\alpha[220]$	Si[110]	-0.73	0.57	1.02
i.14	$\alpha(010)$	Si(3-3-1)	$\alpha[201]$	Si[110]	-2.97	0.54	4.60
i.15	$\alpha(0-10)$	Si(3-3-1)	$\alpha[201]$	Si[110]	-2.97	0.54	4.60
i.16	$\alpha(-234)$	Si(3-3-1)	$\alpha[201]$	Si[110]	-2.97	0.54	4.96
i.17	$\alpha(1-1-3)$	Si(3-3-1)	$\alpha[220]$	Si[110]	-0.73	0.54	4.60
i.18	$\alpha(-2-34)$	Si(3-3-1)	$\alpha[201]$	Si[110]	-2.97	0.54	4.96
i.19	$\alpha(3-3-2)$	Si(3-3-1)	$\alpha[220]$	Si[110]	-0.73	0.54	2.85
i.20	$\alpha(1-1-10)$	Si(1-1-5)	$\alpha[220]$	Si[110]	-0.73	0.52	0.79

Table S4 Top 20 (of 2559) predicted coherent interfaces between silicon and $\gamma\text{-FeSi}_2$ iron silicide (raw data).

Ranking number	(hkl)	(hkl)	[uvw]	[uvw]	δ_1 , close-packed direction misfit, %	R, NCS density	$\tilde{\varepsilon}$, strain, %
$\gamma\text{-FeSi}_2 \parallel \text{Si}$							
i.1	$\gamma(001)$	Si(001)	$\gamma[110]$	Si[110]	-0.77	0.75	0.67
i.2	$\gamma(1-1-1)$	Si(1-1-1)	$\gamma[110]$	Si[110]	-0.77	0.75	0.67
i.3	$\gamma(001)$	Si(001)	$\gamma[100]$	Si[100]	-0.77	0.75	0.67
i.4	$\gamma(1-1-3)$	Si(1-1-3)	$\gamma[110]$	Si[110]	-0.77	0.59	0.67
i.5	$\gamma(-113)$	Si(-113)	$\gamma[411]$	Si[411]	-0.77	0.59	0.67
i.6	$\gamma(-131)$	Si(-131)	$\gamma[411]$	Si[411]	-0.77	0.59	0.67
i.7	$\gamma(0-12)$	Si(0-12)	$\gamma[100]$	Si[100]	-0.77	0.54	0.67
i.8	$\gamma(3-3-1)$	Si(3-3-1)	$\gamma[110]$	Si[110]	-0.77	0.54	0.67
i.9	$\gamma(1-1-5)$	Si(1-1-5)	$\gamma[110]$	Si[110]	-0.77	0.52	0.67
i.10	$\gamma(-15-1)$	Si(-15-1)	$\gamma[411]$	Si[411]	-0.77	0.52	0.67
i.11	$\gamma(-1-15)$	Si(-1-15)	$\gamma[411]$	Si[411]	-0.77	0.52	0.67
i.12	$\gamma(0-13)$	Si(001)	$\gamma[100]$	Si[100]	-0.77	0.51	2.03
i.13	$\gamma(5-5-1)$	Si(5-5-1)	$\gamma[110]$	Si[110]	-0.77	0.50	0.67
i.14	$\gamma(5-5-3)$	Si(5-5-3)	$\gamma[110]$	Si[110]	-0.77	0.50	0.67
i.15	$\gamma(3-3-5)$	Si(3-3-5)	$\gamma[110]$	Si[110]	-0.77	0.50	0.67
i.16	$\gamma(3-3-7)$	Si(3-3-7)	$\gamma[110]$	Si[110]	-0.77	0.50	0.67
i.17	$\gamma(1-1-7)$	Si(1-1-7)	$\gamma[110]$	Si[110]	-0.77	0.49	0.67
i.18	$\gamma(-1-37)$	Si(-1-37)	$\gamma[411]$	Si[411]	-0.77	0.49	0.67
i.19	$\gamma(-122)$	Si(-122)	$\gamma[411]$	Si[411]	-0.77	0.49	0.67
i.20	$\gamma(2-2-1)$	Si(2-2-1)	$\gamma[110]$	Si[110]	-0.77	0.49	0.67

Table S5 Top 20 (of 2713) predicted coherent interfaces between $\beta\text{-FeSi}_2$ and $\alpha\text{-FeSi}_2$ iron silicides (raw data).

Ranking number	(hkl)	(hkl)	[uvw]	[uvw]	δ_1 , close-packed direction misfit, %	R, NCS density	$\tilde{\varepsilon}$, strain, %
$\beta\text{-FeSi}_2 \parallel \alpha\text{-FeSi}_2$							
i.1	$\beta(001)$	$\alpha(-110)$	$\beta[100]$	$\alpha[002]$	-4.01	1.00	1.81
i.2	$\beta(00-1)$	$\alpha(1-10)$	$\beta[010]$	$\alpha[220]$	2.29	1.00	1.81
i.3	$\beta(001)$	$\alpha(-110)$	$\beta[120]$	$\alpha[442]$	0.36	1.00	1.81
i.4	$\beta(00-1)$	$\alpha(1-10)$	$\beta[120]$	$\alpha[442]$	0.36	1.00	1.81
i.5	$\beta(0-10)$	$\alpha(-110)$	$\beta[100]$	$\alpha[002]$	-4.01	1.00	1.83
i.6	$\beta(010)$	$\alpha(1-10)$	$\beta[001]$	$\alpha[220]$	2.78	1.00	1.83
i.7	$\beta(100)$	$\alpha(001)$	$\beta[011]$	$\alpha[400]$	2.53	1.00	2.14
i.8	$\beta(-100)$	$\alpha(00-1)$	$\beta[001]$	$\alpha[220]$	2.78	1.00	2.14
i.9	$\beta(-100)$	$\alpha(001)$	$\beta[011]$	$\alpha[400]$	2.53	1.00	2.14
i.10	$\beta(100)$	$\alpha(00-1)$	$\beta[010]$	$\alpha[220]$	2.29	1.00	2.14
i.11	$\beta(100)$	$\alpha(010)$	$\beta[010]$	$\alpha[201]$	4.65	1.00	4.22
i.12	$\beta(-100)$	$\alpha(0-10)$	$\beta[011]$	$\alpha[400]$	2.53	1.00	4.22
i.13	$\beta(100)$	$\alpha(0-10)$	$\beta[011]$	$\alpha[400]$	2.53	1.00	4.22
i.14	$\beta(100)$	$\alpha(0-10)$	$\beta[010]$	$\alpha[201]$	4.65	1.00	4.22
i.15	$\beta(0-11)$	$\alpha(010)$	$\beta[100]$	$\alpha[002]$	-4.01	0.95	1.82
i.16	$\beta(01-1)$	$\alpha(0-10)$	$\beta[011]$	$\alpha[400]$	2.53	0.95	1.82
i.17	$\beta(-110)$	$\alpha(1-1-2)$	$\beta[001]$	$\alpha[220]$	2.78	0.90	1.19
i.18	$\beta(0-21)$	$\alpha(-130)$	$\beta[100]$	$\alpha[002]$	-4.01	0.90	1.83
i.19	$\beta(11-1)$	$\alpha(0-11)$	$\beta[011]$	$\alpha[400]$	2.53	0.90	1.28
i.20	$\beta(-130)$	$\alpha(3-3-2)$	$\beta[001]$	$\alpha[220]$	2.78	0.86	1.68

Table S6 Top 20 (of 901) predicted coherent interfaces between $\beta\text{-FeSi}_2$ and $\gamma\text{-FeSi}_2$ iron silicides (raw data).

Ranking number	(hkl)	(hkl)	[uvw]	[uvw]	δ_1 , close-packed direction misfit, %	R, NCS density	$\tilde{\varepsilon}$, strain, %
$\beta\text{-FeSi}_2 \parallel \gamma\text{-FeSi}_2$							
i.1	$\beta(100)$	$\gamma(001)$	$\beta[010]$	$\gamma[110]$	2.33	1	2.17
i.2	$\beta(-100)$	$\gamma(001)$	$\beta[011]$	$\gamma[200]$	2.57	1	2.17
i.3	$\beta(-100)$	$\gamma(00-1)$	$\beta[001]$	$\gamma[110]$	2.82	1	2.17
i.4	$\beta(100)$	$\gamma(001)$	$\beta[011]$	$\gamma[200]$	2.57	1	2.17
i.5	$\beta(00-1)$	$\gamma(1-10)$	$\beta[010]$	$\gamma[110]$	2.33	1	4.12
i.6	$\beta(00-1)$	$\gamma(01-1)$	$\beta[120]$	$\gamma[222]$	-1.1	1	4.12
i.7	$\beta(001)$	$\gamma(-110)$	$\beta[120]$	$\gamma[222]$	-1.1	1	4.12
i.8	$\beta(-11-1)$	$\gamma(0-12)$	$\beta[011]$	$\gamma[200]$	2.57	0.95	2.83
i.9	$\beta(-110)$	$\gamma(1-1-1)$	$\beta[001]$	$\gamma[110]$	2.82	0.95	2.13
i.10	$\beta(-310)$	$\gamma(1-1-3)$	$\beta[001]$	$\gamma[110]$	2.82	0.88	1.5
i.11	$\beta(31-1)$	$\gamma(0-23)$	$\beta[011]$	$\gamma[200]$	2.57	0.88	1.13
i.12	$\beta(2-10)$	$\gamma(-12-1)$	$\beta[120]$	$\gamma[222]$	-1.1	0.87	1.19
i.13	$\beta(51-1)$	$\gamma(0-25)$	$\beta[011]$	$\gamma[200]$	2.57	0.86	1.61
i.14	$\beta(-53-3)$	$\gamma(0-56)$	$\beta[011]$	$\gamma[200]$	2.57	0.86	1.7
i.15	$\beta(71-1)$	$\gamma(0-27)$	$\beta[011]$	$\gamma[200]$	2.57	0.86	1.86
i.16	$\beta(-510)$	$\gamma(1-1-5)$	$\beta[001]$	$\gamma[110]$	2.82	0.86	1.88
i.17	$\beta(-210)$	$\gamma(1-1-2)$	$\beta[001]$	$\gamma[110]$	2.82	0.86	1.19
i.18	$\beta(2-1-1)$	$\gamma(-110)$	$\beta[120]$	$\gamma[222]$	-1.1	0.85	1.34
i.19	$\beta(2-11)$	$\gamma(01-1)$	$\beta[120]$	$\gamma[222]$	-1.1	0.85	1.34
i.20	$\beta(-21-1)$	$\gamma(0-11)$	$\beta[011]$	$\gamma[200]$	2.57	0.85	1.34

Table S7 Top 20 (of 10571) predicted coherent interfaces between α -FeSi₂ and γ -FeSi₂ iron silicides (raw data).

Ranking number	(hkl)	(hkl)	[uvw]	[uvw]	δ_1 , close-packed direction misfit, %	R, NCS density	$\tilde{\epsilon}$, strain, %
α -FeSi ₂ γ -FeSi ₂							
i.1	$\alpha(00-1)$	$\gamma(00-1)$	$\alpha[220]$	$\gamma[110]$	0.04	1.00	0.03
i.2	$\alpha(001)$	$\gamma(001)$	$\alpha[200]$	$\gamma[100]$	0.04	1.00	0.03
i.3	$\alpha(010)$	$\gamma(00-1)$	$\alpha[201]$	$\gamma[110]$	-2.22	1.00	2.37
i.4	$\alpha(0-10)$	$\gamma(001)$	$\alpha[200]$	$\gamma[100]$	0.04	1.00	2.37
i.5	$\alpha(010)$	$\gamma(001)$	$\alpha[001]$	$\gamma[100]$	-4.54	1.00	2.37
i.6	$\alpha(0-10)$	$\gamma(00-1)$	$\alpha[201]$	$\gamma[110]$	-2.22	1.00	2.37
i.7	$\alpha(1-10)$	$\gamma(1-10)$	$\alpha[220]$	$\gamma[110]$	0.04	1.00	2.37
i.8	$\alpha(1-10)$	$\gamma(01-1)$	$\alpha[221]$	$\gamma[111]$	-1.46	1.00	2.37
i.9	$\alpha(-110)$	$\gamma(-110)$	$\alpha[221]$	$\gamma[111]$	-1.46	1.00	2.37
i.10	$\alpha(-110)$	$\gamma(0-11)$	$\alpha[223]$	$\gamma[311]$	-3.69	1.00	2.37
i.11	$\alpha(-110)$	$\gamma(0-11)$	$\alpha[001]$	$\gamma[100]$	-4.54	1.00	2.37
i.12	$\alpha(1-10)$	$\gamma(01-1)$	$\alpha[223]$	$\gamma[311]$	-3.69	1.00	2.37
i.13	$\alpha(-1-12)$	$\gamma(1-1-1)$	$\alpha[201]$	$\gamma[110]$	-2.22	0.92	1.53
i.14	$\alpha(1-1-2)$	$\gamma(1-1-1)$	$\alpha[220]$	$\gamma[110]$	0.04	0.92	1.53
i.15	$\alpha(-120)$	$\gamma(0-12)$	$\alpha[001]$	$\gamma[100]$	-4.54	0.90	2.37
i.16	$\alpha(1-1-8)$	$\gamma(1-1-4)$	$\alpha[220]$	$\gamma[110]$	0.04	0.90	0.22
i.17	$\alpha(-1-18)$	$\gamma(-1-14)$	$\alpha[621]$	$\gamma[311]$	-0.37	0.90	0.22
i.18	$\alpha(3-1-4)$	$\gamma(-23-1)$	$\alpha[221]$	$\gamma[111]$	-1.46	0.90	1.65
i.19	$\alpha(0-13)$	$\gamma(0-23)$	$\alpha[200]$	$\gamma[100]$	0.04	0.90	0.67
i.20	$\alpha(-13-4)$	$\gamma(-13-2)$	$\alpha[221]$	$\gamma[111]$	-1.46	0.90	1.65

S2. Density Functional Calculations setup

To support the application of proposed approach, structural characteristics, energies and the phonon spectra of the phases were calculated in the framework of the density functional theory (DFT) implemented in VASP 5.4.1 program package (Kresse & Furthmüller, 1996; Kresse & Hafner, 1993) using the plane wave basis and the projector augmented wave (PAW) formalism (Blöchl, 1994). In order to accurately calculate the second derivatives of the total energy contributing to the dynamical matrix and, further, to all phonon-related quantities, the cutoff energy of the plane-wave basis E_{cutoff} was set to 750 eV. Also, the sampling of the first Brillouin zone in the reciprocal space was made using the Monkhorst-Pack scheme meshes (Pack & Monkhorst, 1977) with resolution of not lower than $0.017 \frac{2\pi}{\text{Å}}$. The convergence criterion of electronic degrees of freedom minimisation was set to 10^{-7} eV. None of considered phases showed magnetic behaviour at the DFT ground state calculations of ideal cells, and thus all further calculations were non-spin-polarised.

The interfacial energies of α -FeSi₂ and Si were calculated with periodic boundary conditions (PBC) so the phase boundaries were modelled by infinite stack of alternating layers (...| α |Si| α |Si| α |Si|...) and the simulation cells contained two identical interface boundaries. Atomic positions were optimized until the forces acting on them were less than 0.01 eV/ \AA . The translation vector perpendicular to the interface plane was also relaxed, while the in-plane cell

dimensions were fixed at corresponding silicon surface cell dimensions. The size of the plane-wave basis was reduced in the interface energies calculations ($E_{\text{cutoff}} = 400$ eV) in order to mitigate the computational costs, however, the basis reduction affects resulting interface energies by no more than 0.2 %.

The description of the lattice dynamics is known to be very sensitive to the choice of the exchange-correlation functional (Jain & McGaughey, 2015). We used the generalised gradient approximation (GGA) in the PBEsol formulation (Perdew *et al.*, 2008), because it correctly reproduces silicon lattice constant, while other popular functionals (LDA, PW91, PBE and rPBE) give errors of the order of 0.03 Å. We have also compared the results for thermal expansion coefficients for PBE (Perdew *et al.*, 1996) and PBEsol against the experimental data (Ibach, 1969; Okada & Tokumaru, 1984). The PBE functional systematically overestimates the expansion coefficient by 14 % in the ranges $T = 300 - 900$ K, while PBEsol gives an average error of 3.8 %.

S3. Calculation of thermal expansion coefficients

In order to study how the lattice misfits and strain at the interfaces change with temperature one needs to know thermal expansion coefficients for the lattice constants of considered phase. The simplest model to assess these quantities is the quasi-harmonic approximation (QHA). It introduces phonon spectra dependence on the volume (Boyer, 1979; Allen *et al.*, 1969), while the contribution to the total energy from the lattice vibrations depends on the phonon spectrum. Thus, Helmholtz's free energy $F_{\text{QHA}}(T, V)$ can be obtained as a function of temperature and volume. Minimization of $F_{\text{QHA}}(T, V)$ with respect to V at fixed temperature gives equilibrium volume the function of $V(T)$ and the Gibbs free energy. The calculations of phonon spectra and corresponding thermodynamic potentials were carried out using the PHONOPY code (Togo & Tanaka, 2015) and its QHA extension, phonopy-qha (Togo *et al.*, 2010).

The calculation of thermal expansion coefficients for every phase was made in four stages:

i) The unit cell geometry was fully optimised until the maximum values of the forces acting on atoms were less than 0.01 eV/Å and the components of the stress tensor were less than 0.5 kbar.

ii) The optimised cell was scaled to generate a set of cells with different volume. The number of scaled cells was different in each case to cover the possible range of volumes. The scaled cells were again relaxed with respect to atomic coordinates and the cell shape, but with a fixed volume. The ratios of lattice parameter changes (e.g. $\Delta a/\Delta c$ for α -FeSi₂) were found to be constant within the considered volume ranges, and these ratios were later used to restore the anisotropic values of linear expansion coefficients.

iii), the force constants were calculated via finite atomic displacements method ($|\Delta r| = 0.01$ Å) for all volumes to obtain the phonon frequencies. The force constants were calculated in supercells to sample the phonon Brillouin zone q-points, which allows estimating phonon DOS more accurately.

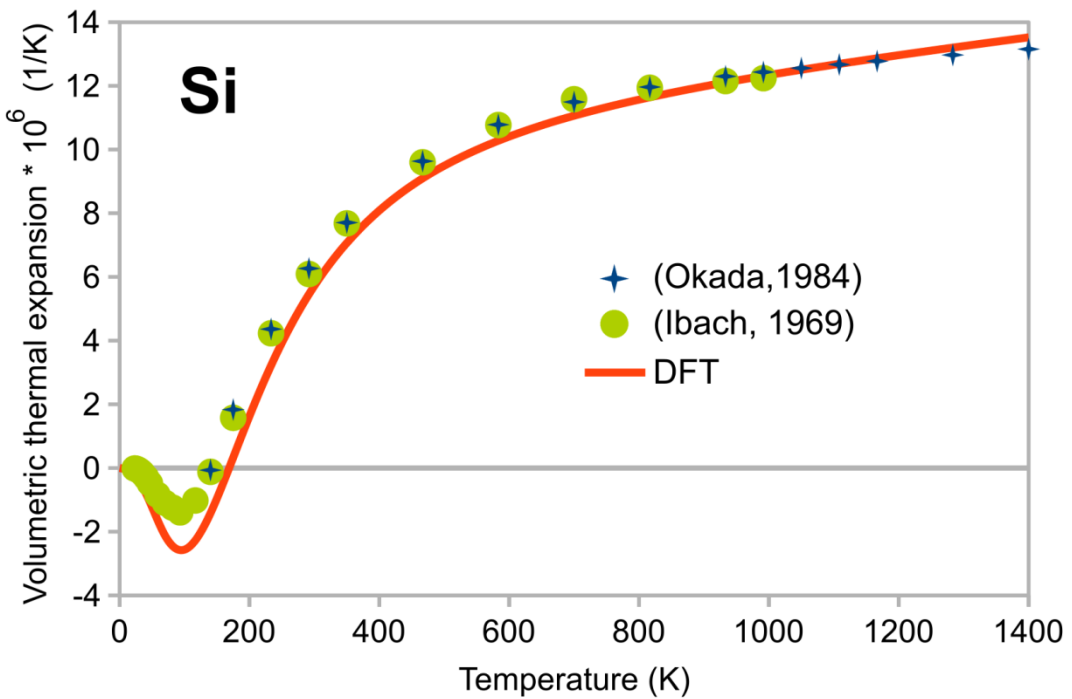
iv) The phonon spectra were used to calculate the thermodynamic potentials and finally determine the $V(T)$ function.

Thermal expansion coefficient of silicon was obtained by calculating 5 different volumes of $2 \times 2 \times 2$ supercell, and the results are in perfect agreement with the experimental data (Fig. S1a).

For $\alpha\text{-FeSi}_2$ 6 different volumes were chosen, the dynamical matrices were calculated with $3 \times 3 \times 2$ supercells for each of them. The calculations of $\beta\text{-FeSi}_2$ started with the primitive cell, rather than the unit cell due to its size. There are 19 irreducible atomic displacements in consideration of low symmetry of the phase, which leads to significantly more computational expenses, than for $\alpha\text{-FeSi}_2$. Thus, the force constants calculations were carried out in $\sqrt{2} \times \sqrt{2} \times 1$ supercell, which coincides with the regular orthorhombic $\beta\text{-FeSi}_2$ unit cell. Five different volumes were used to sample $F_{QHA}(V)$.

For $\gamma\text{-FeSi}_2$ the force constants calculations were carried out in $2 \times 2 \times 2$ supercells with 5 different volumes. At all cell sizes, the phonon spectra showed the presence of imaginary frequencies, which means structural instability and agrees with the fact that this phase has never been observed in bulk. However, there are many reports on its existence in the nanosized form (Zhang & Saxena, 2006), where such destabilising phonon modes are forbidden due to point or boundary defects. Thus, we have discarded these phonon states from the calculations. In order to keep the relation between the number of vibrational modes and the number of atoms, we have renormalized accordingly the contribution of vibrational energy and entropy to the thermodynamic potential, however this have not affected the subsequent qualitative conclusions.

The temperature dependencies of thermal expansion coefficients were compared against available experimental data (Fig. S1.).



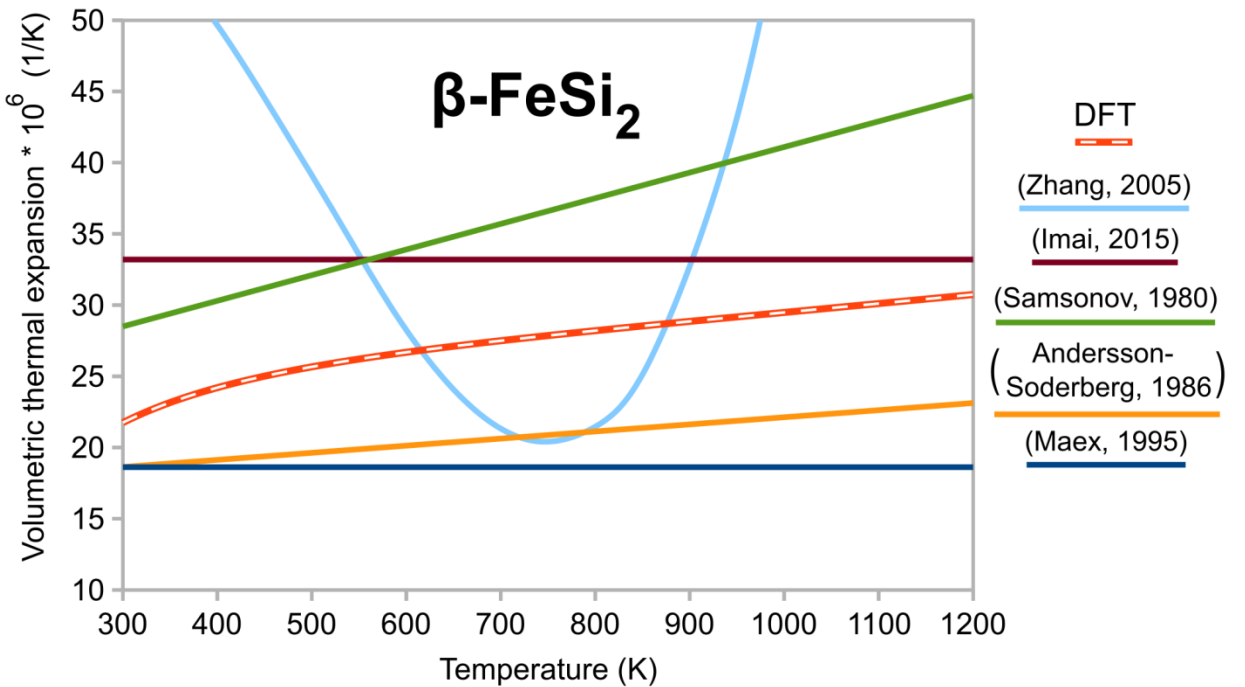
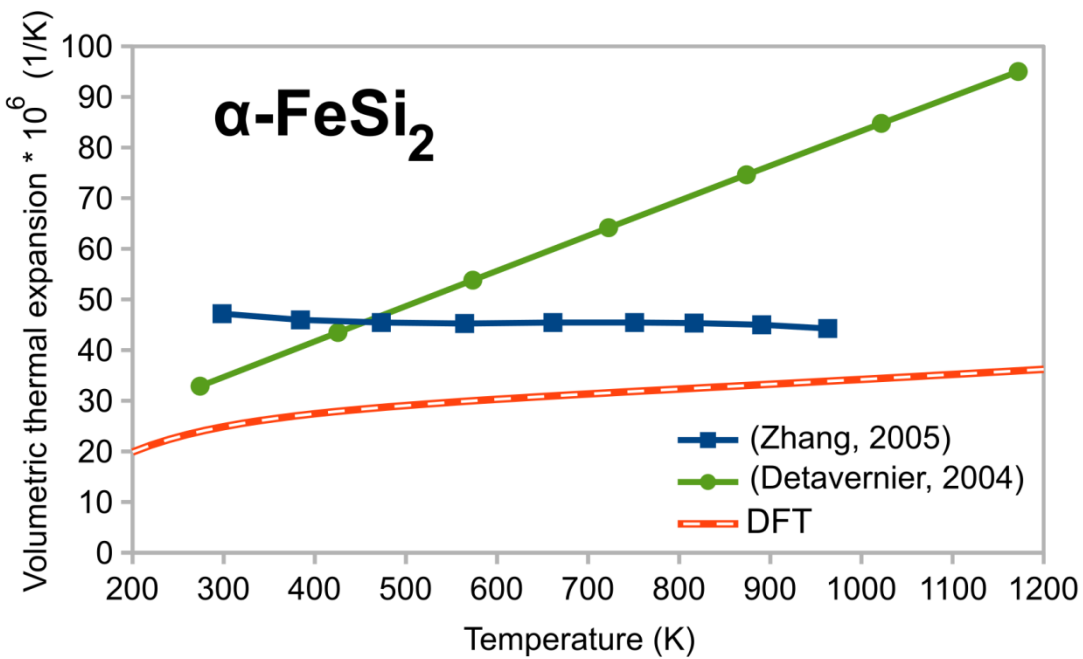


Fig. S1. Volumetric thermal expansion coefficients calculated with DFT (red dashed curves) in comparison with available experimental data [12-19] for a) silicon, b) $\alpha\text{-FeSi}_2$ and c) $\beta\text{-FeSi}_2$.

As can be seen from Fig. S1a, the thermal expansion coefficients calculated for crystalline silicon reproduce well the experimental measurements, especially in high-temperature region. The thermal expansion coefficients for the metastable $\alpha\text{-FeSi}_2$ obtained with QHA are significantly smaller than in two known reports, which is however may be attributed to influence of the substrate (Detavernier *et al.*, 2004) or deviations due to the wider XRD diffraction peaks (Zhang & Saxena, 2006). The agreement of the results for $\beta\text{-FeSi}_2$ with experimental curves should be considered good, while taking into account the discrepancies of the data from the literature itself (Fig. S1c).

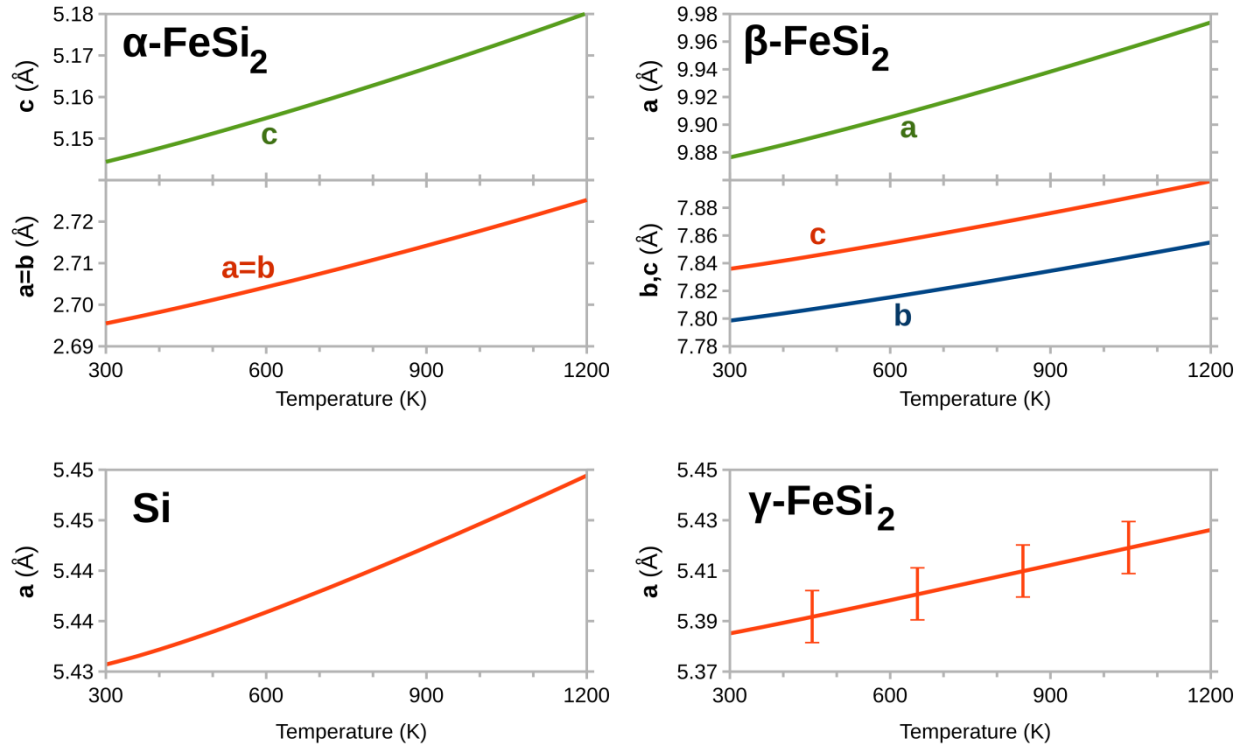


Fig. S2. Temperature dependence of lattice parameters for Si, α -, β - γ -FeSi₂ calculated basing on DFT thermal expansion coefficients and experimental room-temperature lattice constants. See note on γ -FeSi₂ below.

Due to its instability in the bulk, the real lattice constant of standalone γ -FeSi₂ is unknown, so we have estimated the interface strain basing on theoretically calculated lattice constant for γ -FeSi₂. However, the DFT-PBE calculations usually tend to slightly underestimate the lattice constants compared to the experimental ones, e.g. by 0.36 % and 0.75 % for α -FeSi₂ and β -FeSi₂, respectively, thus we have corrected the values obtained for γ -FeSi₂ by 0.36-0.75 %. Therefore, the lattice parameters in Fig. S2 and the strain of the interface between γ and Si in Fig. 6 (γ //Si i.1) are presented with the range marks, corresponding to the upper and the lower limits of the correction.

References:

- Allen, R. E., De Wette, F. W. & Rahman, A. (1969). *Phys. Rev.* **179**, 887–891.
- Andersson-Soderberg, M. (1986). Master Thesis, Uppsala University, Sweden.
- Blöchl, P. E. (1994). *Phys. Rev. B* **50**, 17953–17979.
- Boyer, L. L. (1979). *Phys. Rev. Lett.* **42**, 584–587.
- Detavernier, C., Lavoie, C., Jordan-Sweet, J. & Özcan, A. S. (2004). *Phys. Rev. B* **69**, 174106.
- Ibach, H. (1969). *Phys. Status Solidi* **31**, 625–634.
- Imai, M., Isoda, Y. & Udono, H. (2015). *Intermetallics* **67**, 75–80.
- Jain, A. & McGaughey, A. J. H. (2015). *Comput. Mater. Sci.* **110**, 115–120.
- Kresse, G. & Furthmüller, J. (1996). *Phys. Rev. B* **54**, 11169–11186.

- Kresse, G. & Hafner, J. (1993). *Phys. Rev. B*. **47**, 558–561.
- Maex, K. & van Rossum, M., (1995). *Properties of Metal Silicides*, London: INSPEC.
- Okada, Y. & Tokumaru, Y. (1984). *J. Appl. Phys.* **56**, 314–320.
- Pack, J. D. & Monkhorst, H. J. (1977). *Phys. Rev. B*. **16**, 1748–1749.
- Perdew, J. P., Burke, K. & Ernzerhof, M. (1996). *Phys. Rev. Lett.* **77**, 3865–3868.
- Perdew, J. P., Ruzsinszky, A., Csonka, G. I., Vydrov, O. A., Scuseria, G. E., Constantin, L. A., Zhou, X. & Burke, K. (2008). *Phys. Rev. Lett.* **100**, 136406.
- Samsonov, G. V. & Vinitskii, I. M., (1980). *Handbook of Refractory Compounds*, New York: IFI/Plenum.
- Togo, A., Chaput, L., Tanaka, I. & Hug, G. (2010). *Phys. Rev. B - Condens. Matter Mater. Phys.* **81**, 1–6.
- Togo, A. & Tanaka, I. (2015). *Scr. Mater.* **108**, 1–5.
- Zhang, F. & Saxena, S. (2006). *Scr. Mater.* **54**, 1375–1377.